Article

Evaluating the Impact of Mega-Sports Events on Urbanization Focusing on Land-Use Changes Using a Scenario-Based Model

Jinjin Fan [1,2], Yue Li [3], Wenquan Zhu [4], Yan Chen [1,2], Yao Li [5], Hao Hou [1,2] and Tangao Hu [1,2,*]

1   Institute of Remote Sensing and Geosciences, Hangzhou Normal University, Hangzhou 311121, China; 2019111008006@stu.hznu.edu.cn (J.F.); chenyan_hznu@stu.hznu.edu.cn (Y.C.); houhao@hznu.edu.cn (H.H.)
2   Zhejiang Provincial Key Laboratory of Urban Wetlands and Regional Change, Hangzhou 311121, China
3   Division of Environment and Sustainability, Hong Kong University of Science and Technology, Clear Water Bay, Kowloon, Hong Kong, China; ylijq@connect.ust.hk
4   Faculty of Geographical Science, Beijing Normal University, Beijing 100875, China; zhuwq75@bnu.edu.cn
5   Faculty of Geo-Information Science and Earth Observation (ITC), University of Twente, P.O. Box 217, 7500AE Enschede, The Netherlands; yao.li@utwente.nl
*   Correspondence: hutangao@hznu.edu.cn

Abstract: Mega-sports events have a profound impact on promoting the urbanization process, optimizing the urban spatial structure, and improving the competitiveness of the host city. Taking the 19th Asian Games Hangzhou 2022 (AGH) as an example, we used remote sensing data and a scenario-based model to simulate land-use changes and developments from 2005 to 2025. By setting two scenarios, natural development and AGH-driven development, we explored the impact of AGH on urban development and its driving factors. The results show that (1) cultivated land areas decreased by 369.96 km^2, while construction land areas increased by 488.33 km^2 among the main land-use types in Hangzhou from 2005 to 2020. Urban areas quickly expanded with the West Lake as the center. (2) Urban sprawl intensity under the AGH-driven scenario is expected to increase by 0.91% compared to in the natural-development scenario, indicating that hosting AGH would accelerate the expansion of urban land, particularly in districts set with sports venues such as Binjiang, Xiaoshan, and Yuhang. The strategic trend of supporting the Qiantang River is obvious. (3) Under the influence of AGH, the centroid of urban construction land shifted towards the southeast, and the spatial direction was remarkable. The construction of venues and supporting facilities, and construction land for public rail transit, are the main direct driving forces of urban expansion. The AGH enhances the pace of urbanization, significantly altering the urban spatial structure and helping the city achieve a major transition from the West Lake Era to the Qiantang River Era. Furthermore, our research can provide insights into other cities that will host mega-sports events.

Keywords: mega-sports event; urban development; scenario simulation; driving factors; Hangzhou

Publisher's Note: MDPI stays neutral with regard to jurisdictional claims in published maps and institutional affiliations.

1. Introduction

With the development of society and the economy, urbanization is an inevitable trend and a hot research topic. According to a United Nations (UN) report, the global urban population exceeded the rural population for the first time in 2007 and will increase to 68% of the total global population by 2050 [1]. The expansion rate of construction land is an important indicator to measure urban sprawl and evaluate the urban ecological environment [2]. The simulation of land-use changes and related urban spatial patterns by setting different scenarios is an effective means to explore the process of urban development, providing insights into better adjusting and optimizing urban planning, and helping cities to achieve their future urban construction goals.

In the past few decades, domestic and foreign researchers created many different mathematical models to simulate and predict future land-use development, such as the system dynamic model [3,4], Markov chain model [5], cellular-automata (CA) model [6],

conversion of land-use and its effects (CLUE) [7], agent-based model (ABM) [8], future land-use simulation (FLUS) [9], and geographical simulation and optimization systems (GeoSOS) [10]. Among the different models, CLUE is widely adopted to simulate urban sprawl, land-use/-cover changes, and food safety applications. Verburg [11] optimized CLUE by further improving its simulation speed, accuracy, and convenience of operation, and they proposed the CLUMondo model, which proved effective in many applications, such as simulating global agricultural landscape changes [12] and multiscale land-use/-cover changes [13–16]. These simulation results can also provide useful references to better design policies and incentives to foster greater sustainability on both the global and regional scale.

Mega-sports events are short-term liquidity activities held in a fixed period. While attracting a great number of tourists, holding these events also requires huge economic investments, resulting in long-term and profound impacts on the building environment, economy, and political opportunities of the host city [17,18]. Mega-sports events of sufficient scale and scope affect the whole economy and receive sustained global media attention [19,20]. In addition to the objective benefits to the host city, these include contributing to the promotion of urban regeneration [21], enhancing its international status, repositioning itself in the global tourism market, and gaining an advantage over competitors [22]. For example, they provide the host city with opportunities to improve its urban planning and development, thus accelerating the process of urbanization [23]. The combination of major events and urban planning vigorously promotes urban spatial-structure adjustments, improves the urban environment, and accelerates the pace of urban renewal and transmission [24]. Most promoting effects of holding mega-sports events are related to land-use, such as urban infrastructure, especially transportation network construction [25]. This requires the host city to build new venues and traffic lines, and also to reconfigure urban governance planning and strategic development plans, influencing both the city and its citizens [26]. In previous success cases, such as the Sydney Olympics in 2000 and the London Olympics in 2012, they have successfully transformed the hosting of mega-events into positive drivers of urban development, particularly in terms of infrastructure improvements, urban regeneration, and city branding [22,27]. However, related works focused more on the qualitative evaluation and analysis of driving factors. Combined with the land-use model, our study can better quantitatively simulate and analyze the influence of mega-sports events on urban spatial development.

Taking the 19th Asian Games Hangzhou 2022 (AGH) as a case study, we used a scenario-based model (CLUMondo) to simulate and predict the urban spatial structure under two different scenarios (natural development and AGH-driven development), then we analyzed the potential influencing factors. Our objectives were to (1) monitor historical land-use changes from 2005 to 2020; (2) simulate 2025 Hangzhou land-use changes under the two scenarios; and (3) explore the characteristics of urban land growth, spatial structure, and its driving factors. Our study helps to reveal the influence and driving mechanism of mega-sports events such as AGH on the urban spatial structure of a host city, and it provides the theoretical basis for urban planning and future development in Hangzhou. Furthermore, it is a useful reference for the development planning of other cities hosting mega-sports events.

2. Materials

2.1. Study Area

Hangzhou is located in the north of Zhejiang province, downstream of the Qiantang River (Figure 1), at the geographical coordinates of 29°11′–30°33′ N, 118°21′–120°30′ E. Total land area is around 8260.12 km², of which forestland is around 4676.14 km² (accounting for around 56.61% of the total land area), cultivated land is 1963.58 km² (23.77%), and construction land is 1170.51 km² (14.17%). Hangzhou is the host city of the 19th Asian Games in 2022. Based on previous global experiences of holding mega-sports events by cities, such as the Olympic Games, mega-sports events play a great role in

accelerating the modernization and internationalization of the host city. It also promotes a great transition of Hangzhou's urban planning and development from the West Lake Era towards the Qiantang River Era [28,29]. The land use of the city, however, faces multiple contradictions in terms of rapidly developing the economy and speeding up the urban construction while simultaneously protecting ecosystems and increasing green space. Hence, how to optimize resource allocation on the basis of multiple objectives and deal with contradictions with regard to all parties is a major challenge.
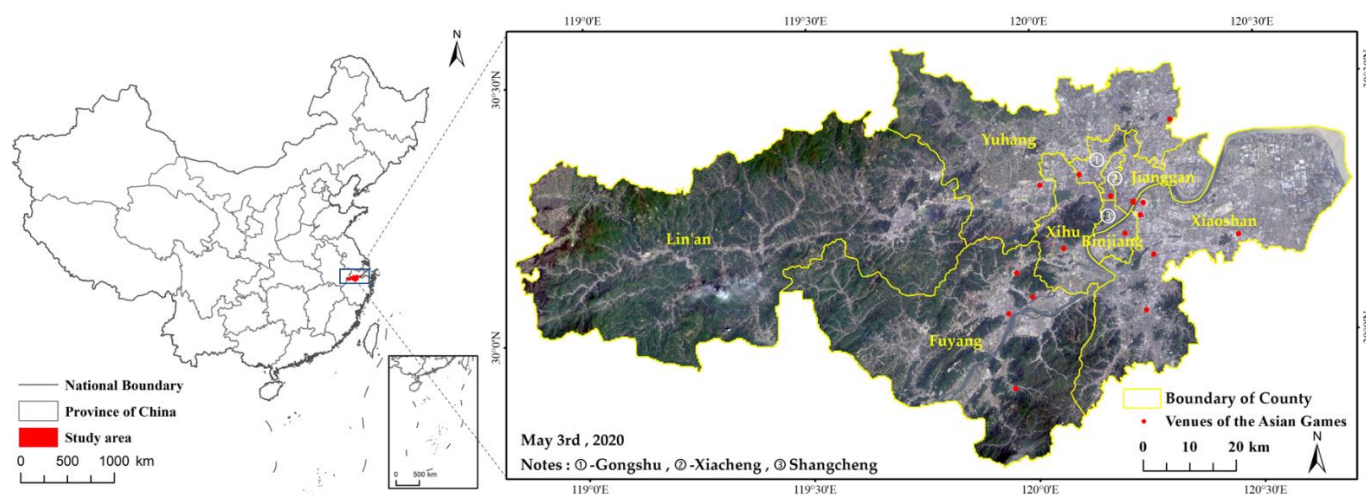

Figure 1. The geographical location of Hangzhou.

2.2. Data

Our data sources were mainly (1) land-use data (Figure 2) consisting of four series (2005, 2010, 2015, and 2018; 30 m spatial resolution) obtained from the Geographical Information Monitoring Cloud Platform (http://www.dsac.cn/). We modified 2018 classification data through artificial visual interpretation, updated them to the interpreted 2020 land-use data, verified data quality by combining field investigations, and randomly selecting dynamic spots for repeated interpretation and analysis. As a result, classification accuracy of cultivated land was 85%, and it could reach more than 75% for the other data, which met the experiment accuracy requirement. (2) A digital elevation model (DEM) was obtained from Geospatial Data Cloud (http://www.gscloud.cn/), on the basis of which we extracted both land slope and aspect. (3) Administrative boundaries, roads, rivers, and city centers were obtained from the National Geomatics Center of China. (4) Per capita GDP was obtained from the 2016 Hangzhou Statistical Yearbook [30] and converted to the raster layer. (5) Population density was from LandScan, a statistical analysis database of global population dynamics (spatial resolution of about 1 km) developed by the Oak Ridge National Laboratory (ORNL).

We resampled all raster data to 1 km as inputs to CLUMondo, and we conducted the simulation using 100 m as an interval. Lastly, the minimal spatial resolution scale suitable for the CLUMondo model was calculated to be 150 m [16].
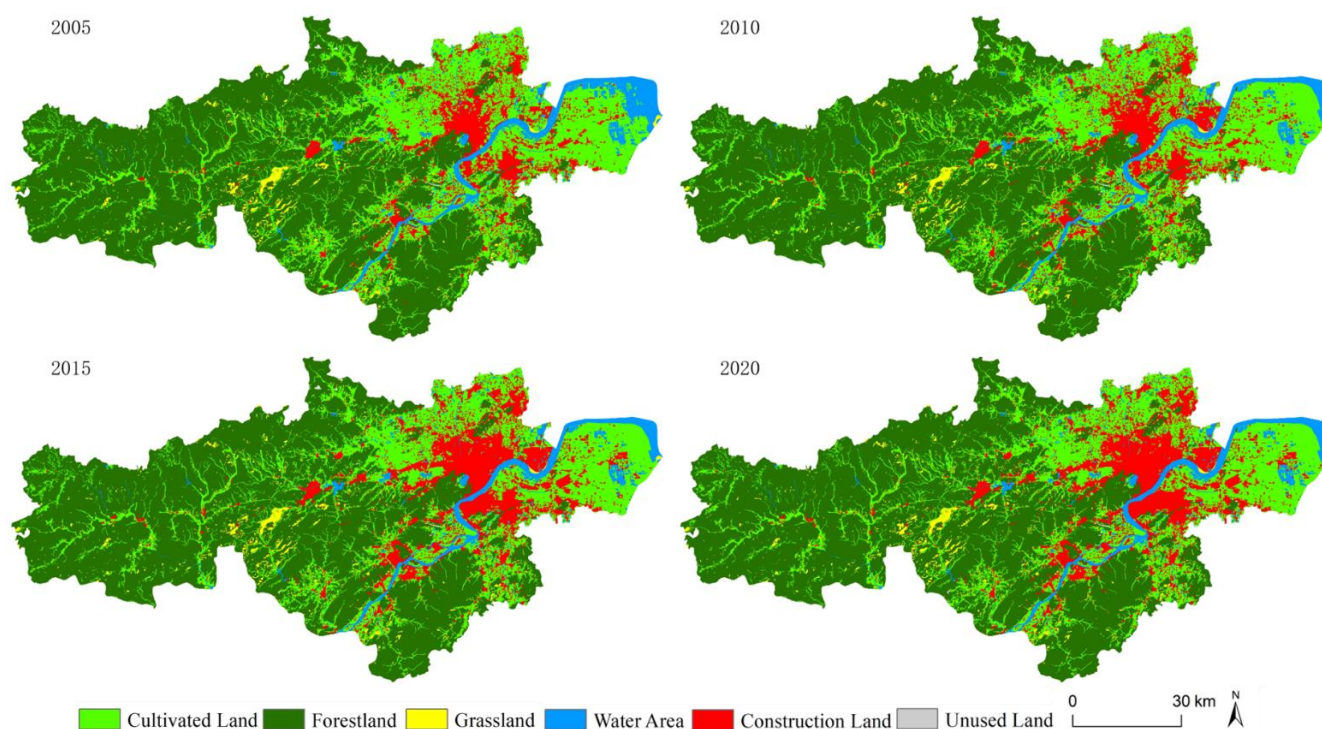
Figure 2. Land use maps of Hangzhou from 2005 to 2020.

3. Methods

This study comprises three parts, namely, CLUMondo model simulation, urban-expansion analysis, and driving-factor analysis (Figure 3). First, to build up the CLU-Mondo model, driving factors were properly selected, model parameters were set, and the urban spatial structure was simulated under different scenarios of natural development and AGH-driven development, respectively. Next, differences between two developing scenarios were analyzed on the basis of indices of urban land-expansion intensity, centroid, and dispersion. Lastly, we discussed the impact of direct driving factors (e.g., venues and supporting facilities, and public transport land) and indirect driving factors (e.g., socioeconomic factors, policy and planning) on urban spatial development.

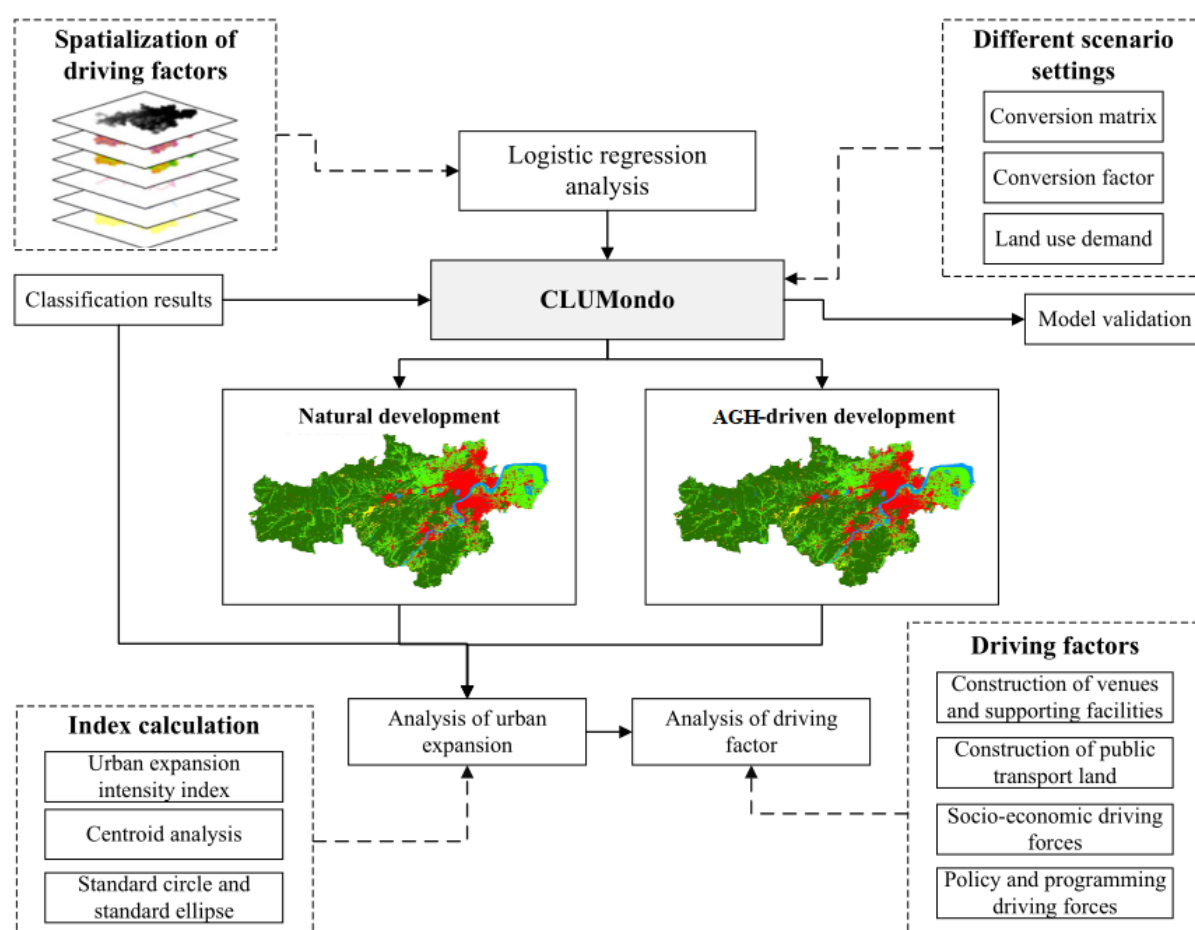**Figure 3.** Flowchart of the study.

3.1. CLUMondo Construction and Setup

CLUMondo is a dynamic and spatially intuitive land-use model, which is the latest addition in the series of models that started as the Conversion of Land Use and its Effects modelling framework (CLUE) [31]. It is an empirical land-use model based on location-suitability analysis that combines the spatiotemporal dynamic competition and interaction dynamic simulation of land-use systems [32]. This model can be divided into the nonspatial demand module and spatial display allocation module, of which the former generates the needed transformation on the system level, such as construction land area and grain output; the latter reveals land-use changes in a specific location of the study area [12]. In this model, external system input is the demand; the allocation algorithm supported by the user interface determines the final allocation result. Specific settings of parameters were as follows.

(1) Adding exclusion layers. Area restriction files can be used to indicate where land-use changes are not allowed. Xixi Wetland and West Lake Scenic Area are natural protected areas in Hangzhou [33], so they are considered as restricted development areas in the model.

(2) Driving-factor selection and validation. Natural geographical elements (e.g., topography) primarily determine land-use/-cover types, and they affect anthropogenic activities, which further influence the conversion of land use patterns and the probability of land use change; socioeconomic factors (e.g., traffic, economy, and population) and relevant policies (e.g., government planning) accelerate the process of land-use/-cover changes. All these elements are land-use change-related driving factors. More importantly, the drivers required by the model either remain relatively stable or change in a jump rather

than an incremental manner over the study period [34]. According to the location factors selected by Liu et al. [35] and Gong et al. [36], considering data collinearity, availability, and quantification [37], we selected 10 driving factors, listed in Table 1.

Table 1. Driving factors descriptions.

IDs	Types	Variable Names	Descriptions
0	Num	DEM	Digital elevation mode
1	Num	Slope	Slope
2	Num	Aspect	Aspect
3	Num	Railway	Distance of each cell to nearest railway or expressway
4	Num	Road	Distance of each cell to nearest main road
5	Num	Subway	Distance of each cell to nearest subway
6	Num	River	Distance of each cell to nearest river
7	Num	Center	Distance of each cell to nearest city center or district center
8	Num	GDP	Per capita GDP
9	Num	Population	Population density

(3) Conversion resistance and conversion matrix. The conversion-resistance coefficient is related to the reversibility of land-use change, the value of which is in the range of 0 (easy to convert) to 1 (irreversible), and it is determined for each land-use type on the basis of the conversion law and expert knowledge of the past few years [38]. The conversion matrix is used to determine whether the current land-use type can be converted, and to which other types it can be converted, where 0 means that conversion is not allowed, 1 that it is allowed, and 10X that the type of land use can be changed after a certain number of years, shown in Table 2, with rows "from" and columns indicating "to".

Table 2. Conversion resistance and conversion matrix in different scenarios.

	a	b	c	d	e	f	Conversion Resistance	a	b	c	d	e	f	Conversion Resistance
a	1	105	1	1	1	1	0.6	1	105	1	1	1	1	0.52
b	1	1	1	1	1	1	0.85	1	1	1	0	0	0	0.88
c	1	105	1	1	1	1	0.7	1	105	1	0	0	0	0.75
d	1	108	1	1	0	1	0.83	0	0	0	1	0	0	0.85
e	0	0	0	0	1	1	0.9	0	0	0	0	1	0	0.92
f	1	1	1	1	1	1	0.3	1	1	1	1	1	1	0.2
Scenario	Natural development							AGH-driven development						

Note: a, cultivated land; b, forestland; c, grassland; d, water areas; e, construction land; f, unused land.

(4) Land-use demand calculation. Land-use demand restricted the simulation to meet the total demand of all types of land-use demand, which is relatively independent of the model itself. We often use the historical-trend extrapolation method to calculate recent land-use demand. Taking the land-use data of 2005, 2010, and 2015 as the basic data sources, the linear interpolation method was used to simulate the land-use condition of each year and predict its future land use.

3.2. Logistic Regression Analysis

One of the advantages of CLUMondo is its internal logistic regression analysis model that combines the locations of each land-use type with the map of driving factors. The model was established as below (Equation (1)) by selecting driving factors for each land-use type with the highest correlation and the probability relationship between them [39,40]:

$$Log\{P_i/(1 - P_i)\} = \beta_0 + \beta_1 X_{1i} + \beta_2 X_{2i} + \ldots\ldots + \beta_n X_{ni}, \tag{1}$$

where P_i is the probability of grid cell i converting to a certain land-use type; X represents all driving factors; and β is the regression coefficients calculated by logistic regression analysis between each land-use type and its driving factors.

We used CLUMondo to conduct regression analysis among 6 land-use types and 10 driving factors, listed in Table 3, to explore the relationship between each dependent variable (a certain land-use type) and multiple independent ones (all driving factors). The area under curve (AUC) is an index to measure accuracy, where the closer the value is to 1, the better regression is. AUC values of six land-use types were all greater than 0.75, indicating that our regression results were accurate.

Table 3. Driving-factor regression statistics.

Driving Factors	Parameters	Cultivated Land	Forestland	Grassland	Water Area	Construction Land	Unused Land
Elevation	β	−0.0052	0.0040	–	−0.0110	−0.0070	0.0090
	Exp(β)	0.9948	1.0040	–	0.9890	0.9930	1.0090
Slope	β	−0.1609	0.2074	–	–	−0.1326	–
	Exp(β)	0.8514	1.2305	–	–	0.8758	–
Aspect	β	0.0023	−0.0029	−0.0010	−0.0013	–	–
	Exp(β)	1.0023	0.9971	0.9991	0.9987	–	–
Distance to railway, expressway	β	0.0003	–	–	–	−0.0004	−0.0002
	Exp(β)	1.0003	–	–	–	0.9996	0.9998
Distance to main road	β	–	−0.0002	0.0001	0.0001	−0.0002	−0.0005
	Exp(β)	–	0.9998	1.0001	1.0001	0.9998	0.9995
Distance to subway	β	–	–	0.0001	–	−0.0001	−0.0001
	Exp(β)	–	–	1.0001	–	0.9999	0.9999
Distance to river	β	–	0.0001	0.0001	−0.0002	–	0.0002
	Exp(β)	–	1.0001	1.0001	0.9999	–	1.0002
Distance to city center	β	0.0004	–	−0.0004	−0.0002	−0.0001	–
	Exp(β)	1.0004	–	0.9996	0.9998	0.9999	–
Per capita GDP (ten thousand RMB)	β	−0.0047	−0.0153	−0.0204	0.0071	–	0.0452
	Exp(β)	0.9953	0.9849	0.9798	1.0072	–	1.0462
Population density(person/square kilometer)	β	−0.0004	−0.0002	−0.0002	−0.0002	0.0002	–
	Exp(β)	0.9996	0.9998	0.9998	0.9998	1.0002	–
Constant		−0.2577	−0.2224	−3.1619	−2.0433	0.4301	−12.7826
AUC		0.8853	0.9703	0.7584	0.8974	0.9225	0.8500

3.3. Land-Use Model Validation

In this section, we used the 2010 land-use classification map as the input to CLUMondo, properly set model parameters (shown in Tables 1 and 2), and simulated the 2015 land-use map (Figure 4). Then, by comparing the simulation results (i.e., 2015 land-use map under the natural-development scenario) and the true land-use classification map (i.e., 2015 land-use classification results), we evaluated the accuracy of our model by calculating a confusion matrix, as shown in Table 4. The results show that the simulation accuracy was high for cultivated land, forestland, grassland, water area, and construction land, with producer accuracy of 81.30%, 91.68%, 88.68%, 97.61%, and 85.79%, respectively. However, the simulation accuracy of unused land was relatively low due to its irregular distribution and relatively small area, which is easy to convert to other land-use types and thus hard to predict.
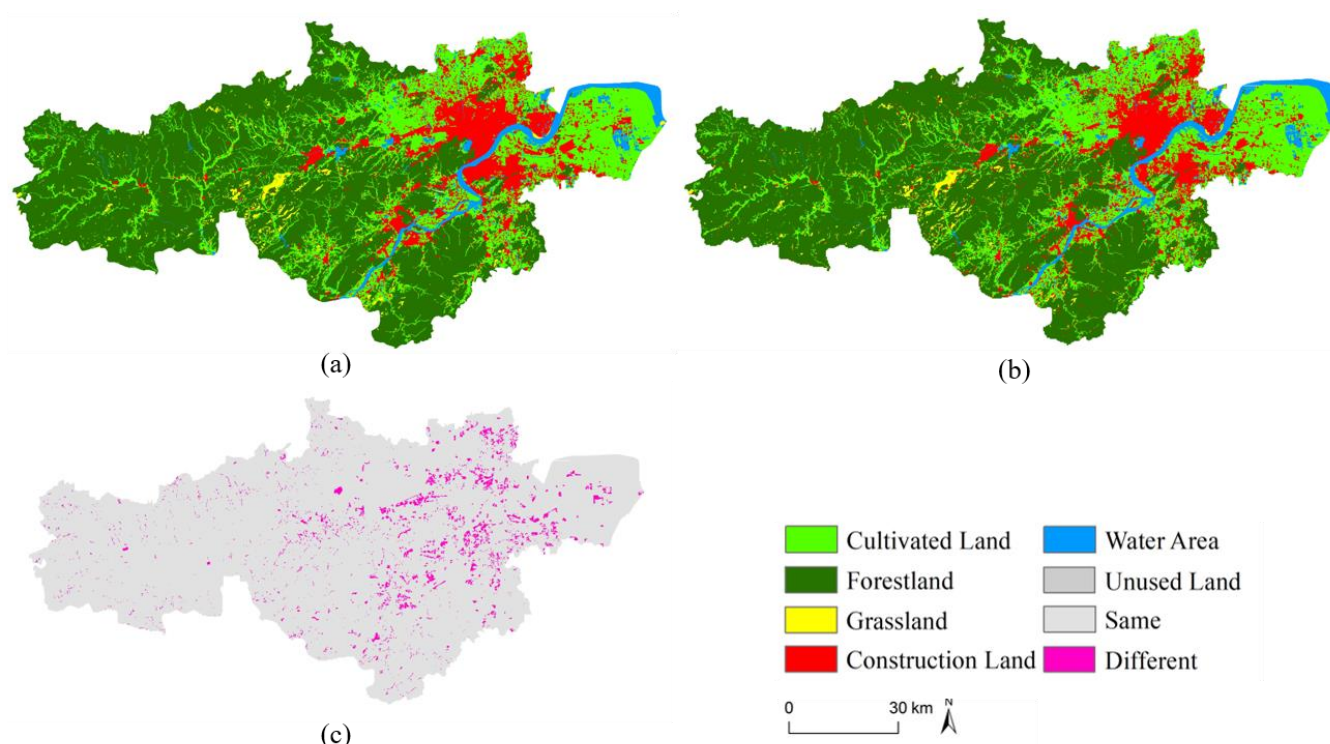
Figure 4. Examinations of land-use modeling results in 2015. (**a**) Actual 2015 classification results; (**b**) simulated 2015 classification results; (**c**) result comparison.

Table 4. The confusion matrix between simulation and observation results.

Observation / Simulation	Cultivated Land	Forestland	Grassland	Water Area	Construction Land	Unused Land	Total
Cultivated land	78,131	13,303	533	124	3948	61	96,100
Forestland	10,542	190,476	1893	967	3886	3	207,767
Grassland	38	0	4519	0	539	0	5096
Water area	121	83	0	14,403	148	0	14,755
Construction land	5103	562	116	313	37,031	41	43,166
Unused land	7	83	0	0	99	44	233
Total	93,942	204,507	7061	15,807	45,651	149	367,117
User accuracy (%)	83.17	93.14	64.00	91.12	81.12	29.53	
Producer accuracy (%)	81.30	91.68	88.68	97.61	85.79	18.88	
Overall classification accuracy (%)				88.42			
Kappa coefficient (%)				80.74			

3.4. Future Development Scenario Setup

In order to reveal land-use changes under different conditions, we designed two scenarios, natural development and AGH-driven development, to simulate future changes. (1) Natural-development scenario: no policy intervention was involved; we calculated the rate of land-use changes on the basis of urban development in the past 10 years (2005–2015) and used this rate to run the following simulations. (2) AGH-driven development scenario: Hangzhou was selected as the host city of 2020 AGH in 2015, and the government thus reissued the Hangzhou Urban Master Plan (2016 revised version) [41] and published the Hangzhou Railway Hub Plan (2016–2030) [42]. AGH is an opportunity for Hangzhou to accelerate the pace of transportation construction (e.g., 4 vertical and 5 horizontal expressways, and 10 subway lines), new city construction (e.g., Asian Games village,

Hangzhou CBD, and Future Science and Technology City) and talent introduction (e.g., West Lake University). Hangzhou also vigorously promoted its urbanization process, with much land planned as construction land and given priority to construct livelihood facilities (such as green spaces and parks). To this end, the annual growth rate of construction land from 2015 to 2020 increased by 0.5% due to AGH compared to that of the 10 previous years.

3.5. Urban Land Expansion Intensity and Difference

The urban expansion intensity index (UEI) refers to the urban expansion intensity in different periods, with its value reflecting corresponding urban expansion situations [43]. The greater the UEI value is, the more intensive and faster urban expansion would be, as per Equation (2):

$$\text{UEI} = (A_{t2} - A_{t1})/(A_{t1} \times \Delta t), \tag{2}$$

where UEI represents urban expansion intensity; A_{t1}, A_{t2} represent urban land area in time t_1 and t_2, respectively; and Δt represents the time interval between t_1 and t_2.

By calculating the area-weighted centroid changes of urban construction land, we can further analyze the law of the development and changes of the urban landscape, and the key trends of urban construction. The calculation of centroids was performed according to Equation (3) [44]:

$$X_C = \left(\sum_{i=1}^{N} C_i X_i \right) / \left(\sum_{i=1}^{N} C_i \right), Y_C = \left(\sum_{i=1}^{N} C_i Y_i \right) / \left(\sum_{i=1}^{N} C_i \right), \tag{3}$$

where X_C and Y_C are the centroid coordinates of urban construction land weighted by area; X_i and Y_i are the centroid coordinates of the ith patch of certain urban construction land; C_i is the area of the ith patch; and n is the total number of patches of urban construction land.

We used the spatial statistics tool in ArcGIS software to calculate the dispersion of urban construction land [45], where the standard circle represents a single summary measure of the distribution of elements around the center; the smaller the radius is, the more concentrated urban distribution would be. The standard deviation ellipse measures the spatial distribution trend of a group of data, and the direction of the long axis represents spatial distribution with the maximal discrete direction. The flattening was calculated from dividing the difference between the major axis and the minor axis by the major axis; the larger the value is, the more obvious the directivity appears.

4. Results

4.1. Land-Use Spatial Structure and Changes

The classification results in Figure 2 show the distribution pattern of different land-use types. For example, the city center is dominated by construction land; most of the eastern and northeastern regions are cultivated land, while the southern and western regions are forestland; Qiantang River passes through the city from northeast to southwest and flows through central built-up areas. The expansion of built-up areas is obvious and mainly comes from the replacement of cultivated land, which gradually expanded from the northwestern bank of the Qiantang River to the southeastern bank. We calculated the area of different land-use types in different years on the basis of classification results (Figure 5), which showed that forestland and grassland rarely changed in the past 15 years; the water area decreased rapidly from 2005 to 2010. This is due to the proximity of the northeastern area of Xiaoshan District to the estuary of the Qiantang River. There are lots of beach resources, formed by the sedimentation of sand from Qiantang River; thus, it has been an important area of reclamation since the last century [46]. During these five years, the reclamation remained very visible, with a large portion converted to cultivated land, followed by a lower decreasing rate. However, the land-use changes of cultivated and construction land are most obvious through the whole ground-feature change process, with cultivated land constantly decreasing and construction land increasing. As a result, cultivated-land area decreased from 2333.54 km^2 (in 2005) to 1963.58 km^2 (in 2020), while

construction land increased from 702.29 km^2 (in 2005) to 1170.51 km^2 (in 2020). Cultivated land decreased at an annual rate of 1.36% from 2010 to 2015, and further to 1.90% from 2015 to 2020. Here, we did not consider the annual reduction rate of cultivated land in the first five years (2005–2010) since it had a large area of reclamation and expansion in this period. However, construction land area increased at an annual rate of 3.30% from 2005 to 2015 and accelerated to 3.80% from 2015 to 2020. In these five years, the total area of construction land increased by nearly 200 km^2, which was mainly converted from cultivated land.
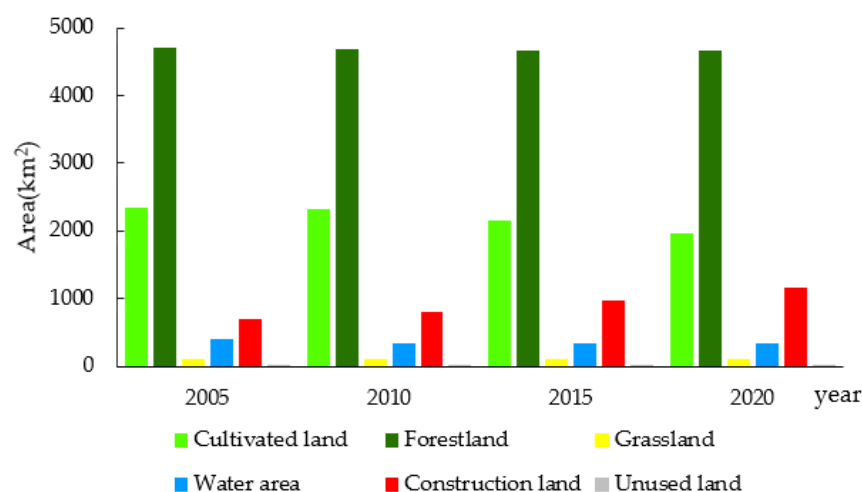

Figure 5. Statistics of land use in Hangzhou from 2005 to 2020 (km^2).

4.2. Scenario Simulation Results

We used CLUMondo to simulate the land-use map of 2025 under two different scenarios on the basis of the historical trend of land-use changes from 2005 to 2015 and from 2015 to 2020 (Figure 6), with the corresponding area statistics shown in Table 5. In the two scenarios, construction land densely occupied the city center, and it continuously expanded by replacing cultivated land.

During the period of 2015–2025 under the natural development scenario, forestland, grassland, and water area generally showed a decreasing trend, where the total reduction in cultivated land was 319.41 km^2, and the increase in construction land was 352.60 km^2, the positions of which coincided with each other. Regarding the AGH-driven scenario, the law of urban growth was similar to that of the natural development scenario, but the expansion rate of construction land and the decreasing rate of cultivated land were higher. During these 10 years, cultivated land was estimated to decrease by 446.31 km^2, and construction land to increase by 441.07 km^2, where main areas for construction land expansion were similar to those in the natural development scenario, but land growth in the districts of Binjiang and Xiaoshan was more intense due to the setting of venues and villages for AGH. The trend of outward expansion from existing construction land was more obvious. Changes in forestland, grassland, and water area were also different. Grassland area decreased at a slow rate from 2005 to 2015, but increased from 2015 in terms of both the 2020 classification results and the 2025 simulation results. However, the areas of forestland and water area slightly increased in 2025 compared to in 2020, which was completely the opposite under the natural development scenario. Land-use change driven by AGH was more remarkable than that under the natural development scenario.
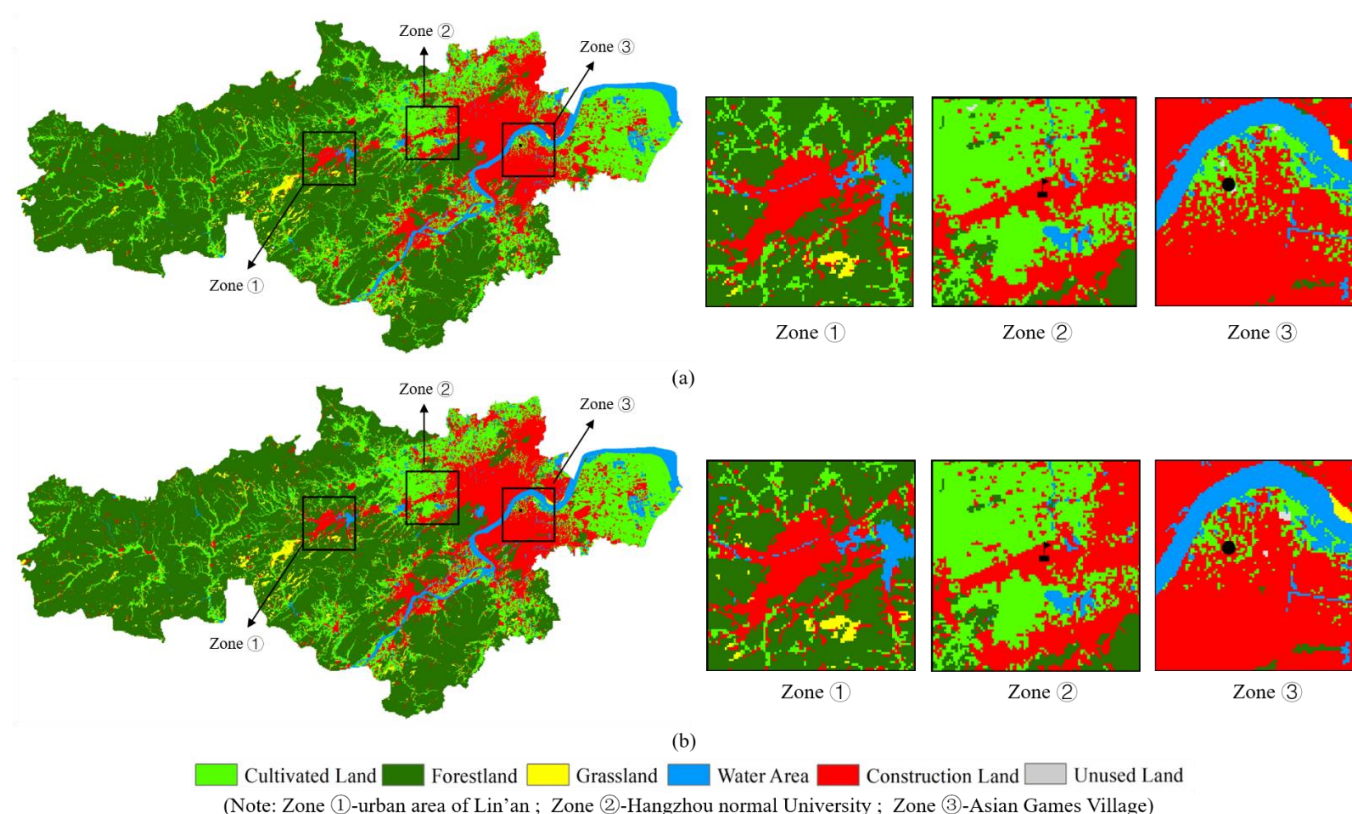
Figure 6. Land-use simulation in 2025. Simulation results of 2025 (**a**) natural development and (**b**) AGH-driven development scenarios.

Table 5. Statistics of simulated land use of Hangzhou in 2025 (km^2).

Scenarios	Cultivated Land	Forestland	Grassland	Water Area	Construction Land	Unused Land
Natural development	1842.84	4659.28	101.54	327.58	1323.83	5.06
AGH-driven development	1715.94	4677.08	119.48	331.92	1412.30	3.42

4.3. Change Detection Results

Figure 7 shows the spatial pattern of different land-use changes from 2005 to 2025, which indicates both the reduction in cultivated land and the increase in construction land. From 2005 to 2015, cultivated land area continuously decreased, and the decrease rate was even higher from 2010 to 2015, mainly concentrated in the periphery of the Xihu, Jianggan, Gongshu, and Binjiang districts and the areas near Xiaoshan International Airport in Xiaoshan district; Lin'an district also showed a small area reduction in its center. On the other hand, the increase in construction land was mostly consistent with the decrease in cultivated land, and there was a strong correlation between them. Under the natural development scenario from 2015 to 2025, cultivated land scattered around existing construction land decreased, while the increase in construction land was mainly concentrated in the eastern part of the Yuhang and Binjiang districts, the central and western regions of Xiaoshan (bordering with Binjiang), and the center of Lin'an. Compared to cultivated land, the increase in construction land was more regular, with few patches. The changing trend under the AGH-driven scenario was similar but more drastic, especially in Binjiang and Xiaoshan, where construction land increased more and faster, expanding along both sides of the Qiantang River.
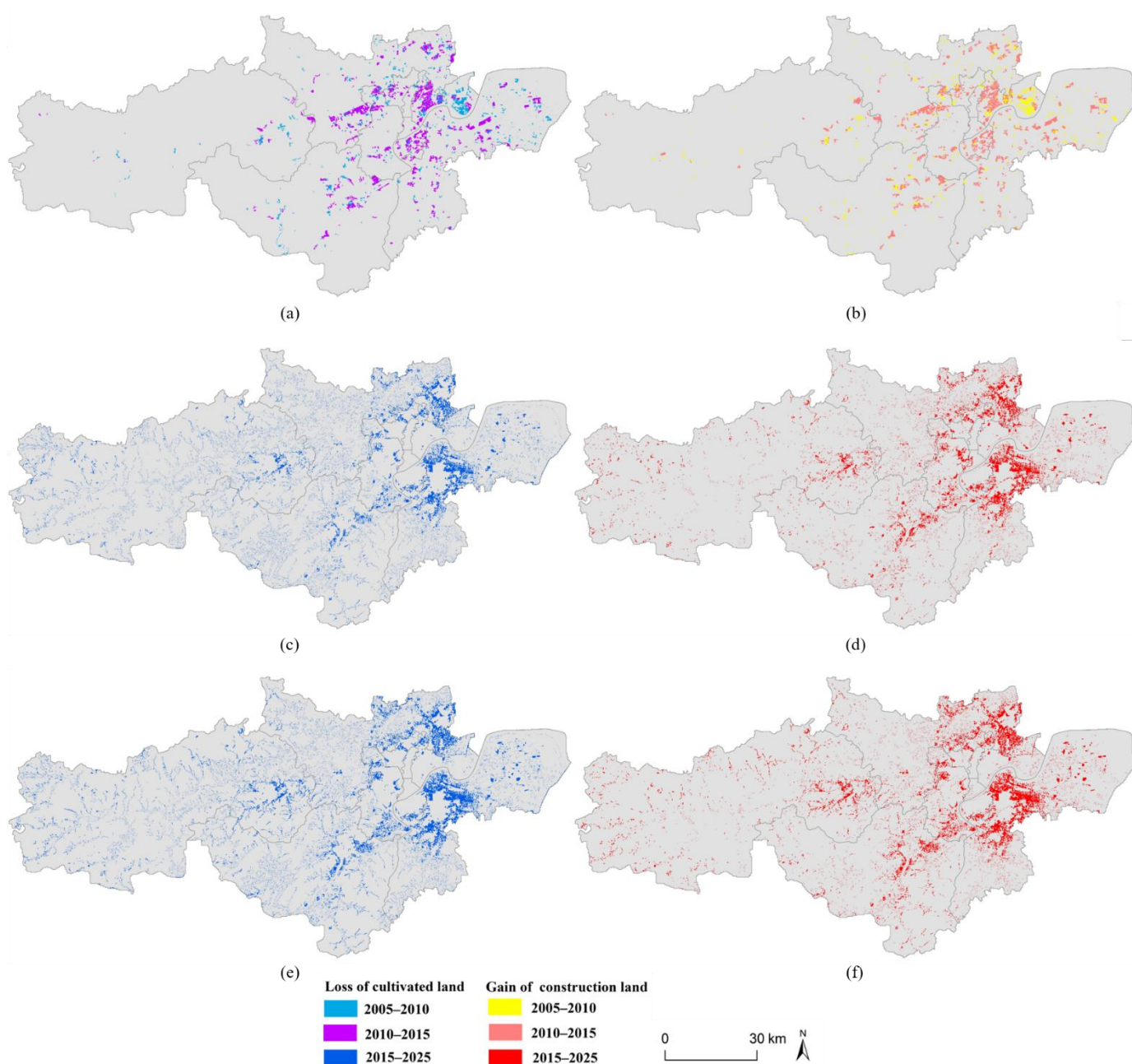
Figure 7. Spatial pattern of land-use changes in study area (2005–2015, 2015–2025). Changes of (**a**) cultivated land from 2005 to 2015, (**b**) construction land from 2005 to 2015, (**c**) cultivated land in the natural development scenario from 2015 to 2025, (**d**) construction land in the natural development scenario from 2015 to 2025, (**e**) cultivated land in the AGH-driven development scenario from 2015 to 2025, and (**f**) construction land in the AGH-driven development scenario from 2015 to 2025.

4.4. Urban Land Expansion Intensity and Difference

The intensity of urban land expansion increased, and urbanization development accelerated. From 2005 to 2010, the intensity index of urban land expansion was the lowest, with a UEI value of 2.88%; in the next five years (2010–2015), the UEI value increased to 4.18%. Due to the rapid development of the city, urban construction land increased rapidly. Specifically, construction land grew 100.98 km^2 from 2005–2015 and 167.97 km^2 from 2010–2015. According to the simulation results, from 2015 to 2025, the UEI value was 3.63% under the natural development scenario, which is slightly lower than that of

the 10 previous years, 3.83%; under the AGH-driven scenario, with more rapid growth of urban construction land, the intensity index was the highest, with a UEI value of 4.54%.

5. Discussion

5.1. Comparative Analysis between Two Scenarios

In the past 15 years, construction land has been continuously expanding, mostly from replacing cultivated land. This observation is consistent with previous studies of cities in China, where urban development has been largely at the expense of the loss of cultivated areas [47–49]. Under the natural development scenario, in addition to cultivated land, some grassland, water area, and forestland also were converted into construction land; in order to implement the concept of "green, intelligent, thrifty and civilized" of AGH, there was even a small increase in grassland and water area under the AGH-driven scenario. Most construction land growth came from the replacement of cultivated land near existing land under both scenarios, and land conversion was more significantly driven by AGH, which the preferable choices of re-use type in the areas were residential land and commercial land [50]. The difference between the two scenarios was that the increase in construction land under the natural development scenario was mainly concentrated east of Yuhang, Binjiang, the central and western areas of Xiaoshan (bordering with Binjiang), and the center of Lin'an. With regard to the AGH-driven scenario, in addition to the increase in the above-mentioned areas, the increase in construction land in Binjiang and Xiaoshan was faster, and the expansion trend along both sides of Qiantang River was obvious.

We analyzed the changes under two scenarios on the basis of three typical regions, shown in Figure 6: Zone 1 is near the urban area of Lin'an, Zone 2 is near the Cangqian campus of Hangzhou Normal University in Yuhang (set with AGH volleyball and rugby venues), and Zone 3 is near the AGH village in Xiaoshan. Through a comparison, construction land was found to mostly grow from existing land, spreading in the form of small spots, and it was more obvious in Zones 1 and 2. Zone 3 is the key area of urban development set with the AGH villages, where constriction land rapidly grew, driven by AGH, covering a large area and dominating this site, which is consistent with reality. Overall, scenario simulation results were highly accurate.

5.2. Urban Spatial Structure Change Analysis

According to the simulation results, in Hangzhou, the change of the centroid of construction land generally shifted towards the southwest, and the shift was more intense under the AGH-driven scenario (Figure 8). Since Lin'an and Fuyang cover large land areas, including a wide area of forestland, which may have caused a deviation in the centroid calculation of the city, we did not consider changes in these two districts. From the results of Hangzhou (excluding Lin'an and Fuyang), the centroid slightly moved towards the southeast, and centroids obtained from two scenarios almost coincided with each other, which was consistent with the concept of supporting the Qiantang River and coordination of the cross-strait economy in Hangzhou [51].

In addition, the oblateness of the standard deviation ellipse, which reflects the change of urban expansion driven construction land, migrated during the study period [49,52]. According to the results based on the standard circle and the standard deviation ellipse, in Hangzhou, the radius and flattening of the standard circle were the largest under the AGH-driven development scenario. So, the urban spatial structure was highly dispersed, and the distribution direction of construction land was the most obvious (Table 6). In Hangzhou excluding Lin'an and Fuyang, the standard circle radius was the largest in 2015, while this value shrank under both the natural development and the AGH-driven development scenarios in 2025, indicating a more concentrated distribution of construction land in this region. However, the flattening value under the AGH-driven development scenario was still the largest (0.24). The overall direction of construction land showed slight dispersion from northwest to southeast. The deflection direction of the standard deviation ellipse of the two different study areas was the opposite because Lin'an and

Fuyang accounted for around 59.30% of the total land area, but forestland was the main land use type, and construction land was scattered, thus leading to the opposite direction in terms of azimuth angle.
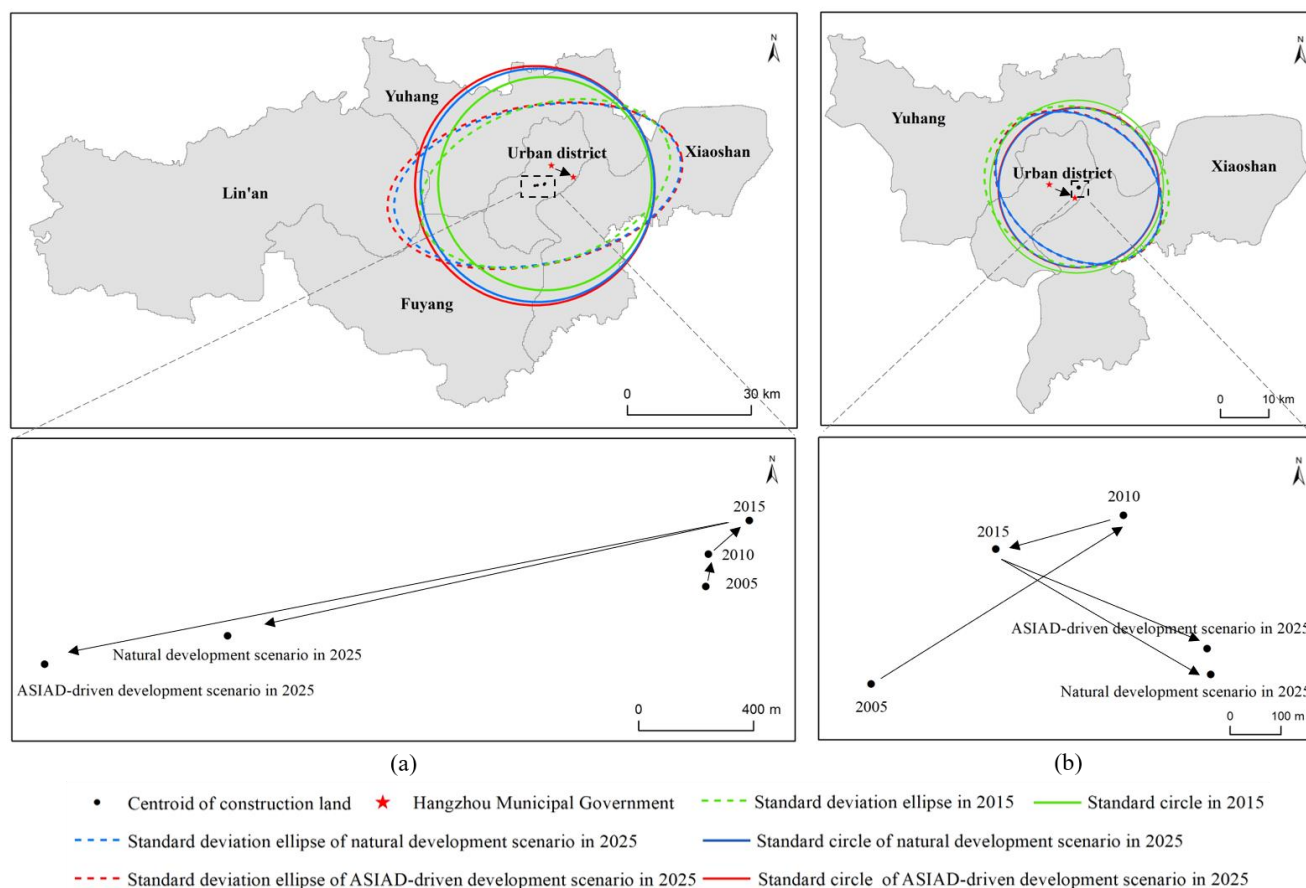

Figure 8. Centroid and dispersion changes in urban construction land (**a**) in Hangzhou, and (**b**) in Hangzhou excluding Lin'an and Fuyang.

Table 6. Information of centroid and dispersion of in urban construction land from 2015 to 2025.

Hangzhou							
Year	CenterX	CenterY	Standard Circle Radius (km)	Standard Deviation Ellipse X	Standard Deviation Ellipse Y	Flattening	Azimuth Angle (°)
2015	802.03	3348.83	25.85	31.22	19.01	0.39	72.00
2025 natural development scenario	800.21	3348.43	28.29	35.20	19.01	0.46	78.40
2025 AGH-drivendevelopment scenario	799.58	3348.33	28.99	36.17	19.29	0.47	78.74
Hangzhou (Excluding Lin'an and Fuyang)							
Year	CenterX	CenterY	Standard Circle Radius (km)	Standard Deviation Ellipse X	Standard Deviation Ellipse Y	Flattening	Azimuth Angle (°)
2015	809.24	3352.79	17.92	19.41	16.29	0.16	110.51
2025 natural development scenario	809.66	3352.54	16.49	18.51	14.19	0.23	125.67
2025 AGH-drivendevelopment scenario	809.65	3352.59	16.65	18.75	14.25	0.24	126.12

5.3. Impact and Driving Factors of Urban Spatial Development

5.3.1. Direct Driving Factors

Holding mega-sports events requires the government to invest a huge amount of labor, material, and money to ensure the smooth implementation of urban construction [53]. According to the contract for the host city [54], Hangzhou will build, renew, or rebuild 33 sporting venues in total, including a new AGH village and an AGH subvillage that, together with supporting facilities, will become the focus of future development in Hangzhou. Taking the venue as the center, it further promotes the increase in surrounding construction land, parks, and other green spaces, and the process of urbanization.

The transportation network is an important factor affecting urban land-use pattern and future scenarios, and planning it plays a leading role in urban development [55]; similarly, rapid urban development promotes the development of transportation networks and the demand for urban rail transit [56], with the two influencing each other. According to the Third Construction Plan of Hangzhou Urban Rail Transit (2017–2022) [57], the Hangzhou Airport Rail Express Line and Hangzhou Metro Line No.1 to 10 will be put into use before 2022. The dense urban rail transit network would strongly support and promote urbanization, and it will accelerate the growth of construction land in Hangzhou. Land-use development near the transportation track is complex, and the growth rate of construction land, such as commercial and residential land, is faster than that of other land-use types [55]. A buffer of 2 km was built for urban rail transit stations, and land-use changes were calculated within the buffer area, as shown in Figure 9, on the basis of which we found that urban rail transit had the greatest impact on construction land and cultivated land. In 2015, construction land accounted for 50.7% of the total buffer area, which will increase to 62.98% and 65.35% under the natural development and AGH-driven development scenarios, respectively, by 2025, mostly via conversion from cultivated land. Urban rail transit can also greatly promote the rapid growth of the surrounding construction land.
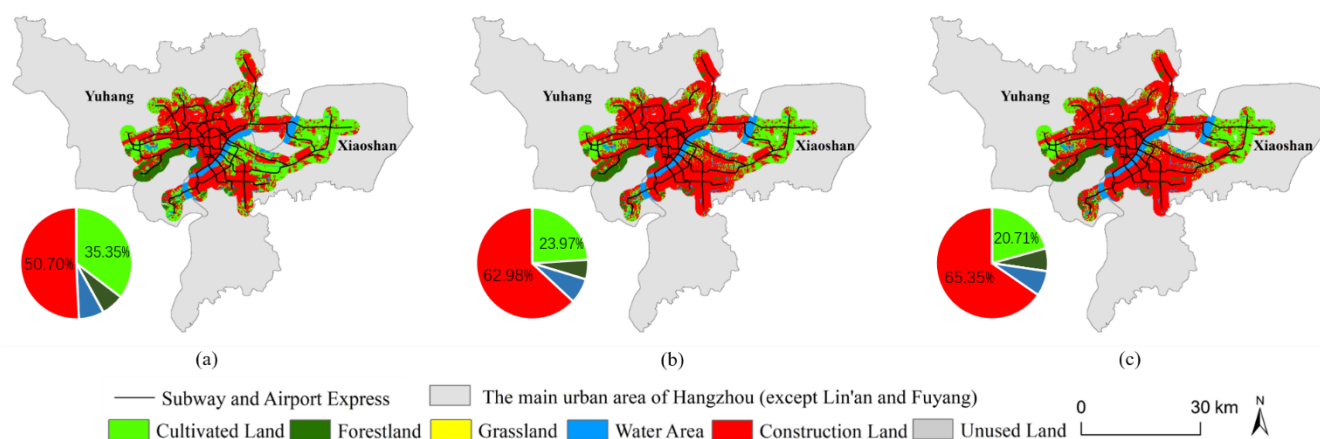

Figure 9. Proportional map of features within 2 km of public rail transit network. (**a**) Classification results in 2015; 2025 simulation results of (**b**) natural development; and (**c**) AGH-driven development scenarios.

5.3.2. Indirect Driving Factors

Mega-sports events effectively promote the growth of urban economic benefits, expand the investment scope of the host city, and increase urban tourism consumption [24]. The construction, holding, and future planning of AGH produce a series of economic benefits to the surrounding venues and promote their economic levels; an improvement in economic development levels can, in turn, have comprehensive and profound impact on land-use changes, positively promoting land development and improving the intensity of land use. The construction phase of AGH will attract many architects and service people that would put greater demand for more construction land for housing, transportation, service

facilities, etc. After that, it will also attract finance, science and technology, and art and culture talent, thus promoting population growth in the city. Meanwhile, the number of tourists will also massively increase. Furthermore, holding the AGH can help to optimize the industrial structure and better achieve the coordinated development of all industries through proper adjustments. Socioeconomic factors such as economic level, population size, and industrial structure indirectly promote urban spatial development.

The spatial pattern of land use is affected by the above driving factors, and also by planning and policies. In order to ensure the successful hosting of the AGH, the Hangzhou municipal government has repeatedly issued relevant planning and policies to determine the overall structure of two cores and eight subs, one ring and eight patches, a balanced network [41] to foster the urbanization construction. In October 2017, venues designed for 34 competition events were determined, the construction of new venues and supporting facilities began in June 2018, and all venues and facilities will be fully completed and put into use by March 2021 [54]. After completing the construction of venues for AGH, policies and planning will guide the direction and speed of urban development [58], improve the transportation system, optimize the urban green environment, and accelerate the growth of residential land and other construction land types, thus having a strong influence on the change of urban spatial structure of the city.

6. Conclusions

In this study, we monitored dynamic changes of historical land use from 2005 to 2020 in Hangzhou, and we used CLUMondo to simulate and predict its future land-use situations in 2025 under the scenarios of natural development and AGH-driven development. We found the following:

1. There were two major land transformation forms according to the analysis of land-use changes from 2005 to 2025; a large area of cultivated land was reduced, and construction land grew fast, accelerating the process of urbanization. In the natural development, cultivated land decreased by 490.70 km^2, and construction land increased by 621.54 km^2. With the AGH-driven development, cultivated land decreased by 617.60 km^2, and construction land increased by 710.01 km^2. Specifically, the increase in construction land will be mainly concentrated in the eastern area of Yuhang, Binjiang, the central and western areas of Xiaoshan (bordering with Binjiang), and the center of Lin'an, with the growth rate particularly rapid in Binjiang and Xiaoshan along both sides of the Qiantang River.
2. With the development and construction of Hangzhou, the centroid of urban construction constantly shifted, which shifted to the southwest with a larger offset driven by AGH. Urban dispersion slightly increased with an obvious spatial direction. However, in Hangzhou (excluding the Lin'an and Fuyang districts), the centroid shifted to the southeast with a similar offset under two different simulation scenarios. Urban dispersion showed a tendency of gathering, but the spatial direction was still obvious.
3. The Hangzhou Government has issued several documents on the construction of the Asian Games and transport [54,57,59,60], which are of great importance in planning city development. The construction and improvement of venues, supporting facilities, and public rail transit are direct driving factors for future urban spatial development; socioeconomic policy and planning indirectly affect urban development by affecting the direct driving factors.

Although our study takes the 19th Asian Games Hangzhou 2022 as an example, it can effectively evaluate the impact of mega-sports events on urbanization process and urban spatial structures based on a scenario-based model, so as to provide insights into other cities that will host mega-sports events.

J.F., T.H. and H.H.; supervision, T.H. and W.Z. All authors have read and agreed to the published version of the manuscript.

References

1. Revision of World Urbanization Prospects. Available online: https://www.un.org/development/desa/publications/2018-revision-of-world-urbanization-prospects.html (accessed on 26 July 2018).
2. El Garouani, A.; Mulla, D.J.; El Garouani, S.; Knight, J. Analysis of urban growth and sprawl from remote sensing data: Case of Fez, Morocco. *Int. J. Sustain. Built Environ.* **2017**, *6*, 160–169. [CrossRef]
3. He, C.; Okada, N.; Zhang, Q.; Shi, P.; Zhang, J. Modeling urban expansion scenarios by coupling cellular automata model and system dynamic model in Beijing, China. *Appl. Geogr.* **2006**, *26*, 323–345. [CrossRef]
4. Rasmussen, L.V.; Rasmussen, K.; Reenberg, A.; Proud, S. A system dynamics approach to land use changes in agro-pastoral systems on the desert margins of Sahel. *Agric. Syst.* **2012**, *107*, 56–64. [CrossRef]
5. Das, S.; Sarkar, R. Predicting the land use and land cover change using Markov model: A catchment level analysis of the Bhagirathi-Hugli River. *Spat. Inf. Res.* **2019**, *27*, 439–452. [CrossRef]
6. Dietzel, C.; Clarke, K. The effect of disaggregating land use categories in cellular automata during model calibration and forecasting. *Comput. Environ. Urban Syst.* **2006**, *30*, 78–101. [CrossRef]
7. Verburg, P.H.; Eickhout, B.; van Meijl, H. A multi-scale, multi-model approach for analyzing the future dynamics of European land use. *Ann. Reg. Sci.* **2007**, *42*, 57–77. [CrossRef]
8. Tian, G.; Ma, B.; Xu, X.; Liu, X.; Xu, L.; Liu, X.; Xiao, L.; Kong, L. Simulation of urban expansion and encroachment using cellular automata and multi-agent system model—A case study of Tianjin metropolitan region, China. *Ecol. Indic.* **2016**, *70*, 439–450. [CrossRef]
9. Liu, X.; Liang, X.; Li, X.; Xu, X.; Ou, J.; Chen, Y.; Li, S.; Wang, S.; Pei, F. A future land use simulation model (FLUS) for simulating multiple land use scenarios by coupling human and natural effects. *Landsc. Urban Plan.* **2017**, *168*, 94–116. [CrossRef]
10. Li, X.; Chen, Y.; Liu, X.; Li, D.; He, J. Concepts, methodologies, and tools of an integrated geographical simulation and optimization system. *Int. J. Geogr. Inf. Sci.* **2010**, *25*, 633–655. [CrossRef]
11. Verburg, P.H.; Overmars, K.P. Combining top-down and bottom-up dynamics in land use modeling: Exploring the future of abandoned farmlands in Europe with the Dyna-CLUE model. *Landsc. Ecol.* **2009**, *24*, 1167–1181. [CrossRef]
12. Van Asselen, S.; Verburg, P.H. Land cover change or land-use intensification: Simulating land system change with a global-scale land change model. *Glob. Chang. Biol.* **2013**, *19*, 3648–3667. [CrossRef] [PubMed]
13. Ornetsmüller, C.; Verburg, P.H.; Heinimann, A. Scenarios of land system change in the Lao PDR: Transitions in response to alternative demands on goods and services provided by the land. *Appl. Geogr.* **2016**, *75*, 1–11. [CrossRef]
14. Huang, J.; Liu, Y.; Zhang, X.; Wang, Y.; Wang, Y. A Scenario-Based Simulation of Land System Changes on Dietary Changes: A Case Study in China. *Sustainability* **2019**, *11*, 5196. [CrossRef]
15. Zhu, W.; Gao, Y.; Zhang, H.; Liu, L. Optimization of the land use pattern in Horqin Sandy Land by using the CLUMondo model and Bayesian belief network. *Sci. Total Environ.* **2020**, *739*, 1–15. [CrossRef]
16. Arunyawat, S.; Shrestha, R.P. Simulating future land use and ecosystem services in Northern Thailand. *J. Land Use Sci.* **2018**, *13*, 146–165. [CrossRef]
17. Caiazza, R.; Audretsch, D. Can a sport mega-event support hosting city's economic, socio-cultural and political development? *Tour. Manag. Perspect.* **2015**, *14*, 1–2. [CrossRef]
18. Müller, M. What makes an event a megaevent Definitions and sizes. *Leis. Stud.* **2017**, *34*, 627–642. [CrossRef]
19. Preuss, H. A framework for identifying the legacies of a mega sport event. *Leis. Stud.* **2015**, *34*, 643–664. [CrossRef]
20. Klement, M. Mega-Events and Globalization. Capital and Spectacle in a Changing World Order. *Hist. Sociol.* **2017**, *2017*, 134–138.
21. Gold, J.R.; Gold, M.M. Land remediation, event spaces and the pursuit of Olympic legacy. *Geogr. Compass* **2020**, *14*, 1–16. [CrossRef]
22. Gold, J.; Gold, M. *Olympic Cities: City Agendas, Planning and the World's Games, 1896–2020*; Routledge: Abingdon, UK, 2016; pp. 1–484.
23. Zhao, S.X.; Ching, J.L.; He, Y.; Chan, N.Y.M. Playing Games and Leveraging on Land: Unfolding the Beijing Olympics and China's Mega-event rbanization Model. *J. Contemp. China* **2016**, *26*, 1–23. [CrossRef]

24. Oja, B.D.; Wear, H.T.; Clopton, A.W. Major Sport Events and Psychic Income: The Social Anchor Effect. *J. Sport Manag.* **2018**, *32*, 257–271. [CrossRef]

25. Parra-Camacho, D.; Añó Sanz, V.; Ayora Pérez, D.; González-García, R.J. Applying importance-performance analysis to residents' perceptions of large sporting events. *Sport Soc.* **2019**, *23*, 249–263. [CrossRef]

26. Müller, M.; Gaffney, C. Comparing the urban impacts of the fifa world cup and olympic games from 2010 to 2016. *J. Sport Soc. Issues* **2018**, *42*, 247–269. [CrossRef]

27. Gold, J.R.; Gold, M.M. Olympic Cities: Regeneration, City Rebranding and Changing Urban Agendas. *Geogr. Compass* **2008**, *2*, 300–318. [CrossRef]

28. Maennig, W.; du Plessis, S. Sport Stadia, Sporting Events and Urban Development: International Experience and the Ambitions of Durban. *Urban Forum.* **2009**, *20*, 61–76. [CrossRef]

29. Pye, P.N.; Toohey, K.; Cuskelly, G. The social benefits in sport city planning: A conceptual framework. *Sport Soc.* **2015**, *18*, 1199–1221. [CrossRef]

30. Hangzhou Statistical Yearbook 2016. Available online: http://tjj.hangzhou.gov.cn/art/2016/9/23/art_1229453592_3819409.html (accessed on 23 September 2016).

31. Verburg, P.H.; De Koning, G.H.J.; Kok, K.; Veldkamp, A.; Bouma, J. A spatial explicit allocation procedure for modelling the pattern of land use change based upon actual land use. *Ecol. Model.* **1999**, *116*, 45–61. [CrossRef]

32. Eitelberg, D.A.; van Vliet, J.; Verburg, P.H. A review of global potentially available cropland estimates and their consequences for model-based assessments. *Glob. Chang. Biol.* **2015**, *21*, 1236–1248. [CrossRef] [PubMed]

33. Hu, T.; Liu, J.; Zheng, G.; Li, Y.; Xie, B. Quantitative assessment of urban wetland dynamics using high spatial resolution satellite imagery between 2000 and 2013. *Sci. Rep.* **2018**, *8*, 1–10. [CrossRef]

34. Van Vliet, J.; Verburg, P.H. A Short Presentation of CLUMondo. In *Geomatic Approaches for Modeling Land Change Scenarios*; Camacho Olmedo, M.T., Paegelow, M., Mas, J.-F., Escobar, F., Eds.; Springer International Publishing: Cham, Switzerland, 2018; pp. 485–492.

35. Liu, Z.; Verburg, P.H.; Wu, J.; He, C. Understanding Land System Change Through Scenario-Based Simulations: A Case Study from the Drylands in Northern China. *Environ. Manag.* **2017**, *59*, 440–454. [CrossRef] [PubMed]

36. Gong, B.; Liu, Z. Assessing impacts of land use policies on environmental sustainability of oasis landscapes with scenario analysis: The case of northern China. *Landsc. Ecol.* **2020**, 1–20. [CrossRef]

37. Aburas, M.M.; Ho, Y.M.; Ramli, M.F.; Ash'aari, Z.H. The simulation and prediction of spatio-temporal urban growth trends using cellular automata models: A review. *Int. J. Appl. Earth Obs. Geoinf.* **2016**, *52*, 380–389. [CrossRef]

38. Shao, J.; Dang, Y.; Wang, W.; Zhang, S. Simulation of future land-use scenarios in the Three Gorges Reservoir Region under the effects of multiple factors. *J. Geogr. Sci.* **2018**, *28*, 1907–1923.

39. Gobin, A.; Campling, P.; Feyen, J. Logistic modelling to derive agricultural land use determinants: A case study from southeastern Nigeria. *Agri. Ecosyst. Environ.* **2002**, *89*, 213–228. [CrossRef]

40. Hu, T.; Liu, J.; Zheng, G.; Zhang, D.; Huang, K. Evaluation of historical and future wetland degradation using remote sensing imagery and land use modeling. *Land Degrad. Dev.* **2019**, *31*, 65–80. [CrossRef]

41. State Council of the PRC. *Urban Master Plan of Hangzhou (2001–2020) (Revised in 2016)*; State Council of the PRC: Beijing, China, 2016.

42. China Railway Corporation; Zhejiang Provincial People's Government. *Reply on Hangzhou Railway Hub Planning (2016–2030)*; Zhejiang Provincial People's Government: Hangzhou, China, 2017.

43. Zhong, Y.; Lin, A.; He, L.; Zhou, Z.; Yuan, M. Spatiotemporal Dynamics and Driving Forces of Urban Land-Use Expansion: A Case Study of the Yangtze River Economic Belt, China. *Remote Sens.* **2020**, *12*, 287. [CrossRef]

44. Fahui, W. *Quantitative Methods and Application in GIS*; CRC Press LLC: Florida, FL, USA, 2006.

45. Qiao, K.; Zhu, W.; Hu, D.; Hao, M.; Chen, S.; Cao, S. Examining the distribution and dynamics of impervious surface in different function zones in Beijing. *J. Geogr. Sci.* **2018**, *28*, 669–684. [CrossRef]

46. Li, J.-T.; Liu, Y.-S.; Yang, Y.-Y. Land use change and effect analysis of tideland reclamation in Hangzhou Bay. *J. Mt. Sci.* **2018**, *15*, 394–405. [CrossRef]

47. Hou, H.; Wang, R.; Murayama, Y. Scenario-based modelling for urban sustainability focusing on changes in cropland under rapid urbanization: A case study of Hangzhou from 1990 to 2035. *Sci. Total Environ.* **2019**, *661*, 422–431. [CrossRef]

48. Zhang, Z.; Li, N.; Wang, X.; Liu, F.; Yang, L. A Comparative Study of Urban Expansion in Beijing, Tianjin and Tangshan from the 1970s to 2013. *Remote Sens.* **2016**, *8*, 1–22. [CrossRef]

49. Tu, Y.; Chen, B.; Yu, L.; Xin, Q.; Gong, P.; Xu, B. How does urban expansion interact with cropland loss? A comparison of 14 Chinese cities from 1980 to 2015. *Landsc. Ecol.* **2020**, *36*, 243–263. [CrossRef]

50. Huang, L.; Shahtahmassebi, A.; Gan, M.; Deng, J.; Wang, J.; Wang, K. Characterizing spatial patterns and driving forces of expansion and regeneration of industrial regions in the Hangzhou megacity, China. *J. Clean. Prod.* **2020**, *253*, 119959. [CrossRef]

51. Action Plan for Qiantang River Development in Hangzhou. Available online: http://www.hangzhou.gov.cn/art/2019/1/5/art_812262_29196169.html (accessed on 5 January 2019).

52. Wang, B.; Shi, W.; Miao, Z. Confidence analysis of standard deviational ellipse and its extension into higher dimensional euclidean space. *PLoS ONE* **2015**, *10*, 1–17. [CrossRef] [PubMed]

53. Dwyer, L.; Forsyth, P.; Spurr, R. Estimating the Impacts of Special Events on an Economy. *J. Travel Res.* **2016**, *43*, 351–359. [CrossRef]

54. Opinions of the Organizing Committee of the 19th Asian Games in 2022 on Speeding up the Construction of Venues and Facilities in Hangzhou for the 19th Asian Games in 2022. Available online: http://www.hangzhou.gov.cn/art/2017/11/13/art_1256295_12962826.html (accessed on 15 October 2017).

55. Bhattacharjee, S.; Goetz, A.R. The rail transit system and land use change in the Denver metro region. *J. Transp. Geogr.* **2016**, *54*, 440–450. [CrossRef]

56. Shen, Q.; Chen, P.; Pan, H. Factors affecting car ownership and mode choice in rail transit-supported suburbs of a large Chinese city. *Transp. Res. Part A Policy Pract.* **2016**, *94*, 31–44. [CrossRef]

57. Construction Plan of the Third Phase of Hangzhou Urban Rail Transit (2017–2022). Available online: https://www.ndrc.gov.cn/xxgk/zcfb/tz/201612/t20161222_962824.html (accessed on 12 December 2016).

58. Lin, G.C.S.; He, C.; Li, X.; Wu, Y. Empowering regional economy with a spectacular space: Mega-events, over-drafted capital and momentary growth in China's metropolises. *Area Dev. Policy* **2017**, *3*, 24–41. [CrossRef]

59. Approval of Hangzhou Municipal People's Government on the Special Planning of Hangzhou Venues and Facilities for the 19th Asian Games. Available online: http://www.hangzhou.gov.cn/art/2020/8/7/art_1229063387_1133741.html (accessed on 7 August 2020).

60. Action Plan for Creating a Model City with Strong Transportation in Hangzhou (2020–2025). Available online: http://www.hangzhou.gov.cn/art/2020/7/20/art_1229063390_3656548.html (accessed on 20 July 2020).